Raw Algerian Calcic Clay as a Sustainable Adsorbent for Pesticide Removal

Feddal Imene[1,2 *], Ben Arraba Imad Eddine [3], Abdelhak Mesbah[2], Mimanne Goussem[2]

[1]Abdel Hamid Ibn Badis University of Mostaganem 27000, Algeria
[2]Laboratory of Materials & Catalysis, Faculty of Exact Sciences Djillali LIABES University (UDL)
[3] Djillali Liabes University of Sidi Bel Abbes 22000, Algeria

[*] Corresponding author, e-mail: fimene22@hotmail.com

Abstract

Pesticides are widely used globally to control weeds and enhance agricultural yields. However, excessive herbicide application causes severe environmental issues, notably leading to biodiversity loss. This study investigates the adsorption of diuron, a persistent phenylurea derivative herbicide widely found in soil as well as ground and surface waters, from an aqueous solution onto raw calcium clay. Characterization analyses of the clay were systematically performed. The adsorption study was optimized by evaluating key influencing parameters, including contact time, adsorbent dosage, pH, and temperature. Furthermore, the experimental equilibrium data were modeled using Langmuir, Freundlich, Temkin, and Elovich isotherms to understand the surface interaction mechanisms. The results demonstrate that the removal of diuron onto raw calcium clay is an exothermic process and aligns well with the Freundlich isotherm model. This work highlights the potential of natural calcium clay as a cost-effective and eco-friendly adsorbent for sustainable wastewater treatment.

Keywords: **Diuron, Adsorption, Calcic Clay, Adsorption Isotherms, Water Treatment.**

1. Introduction

Environmental pollution has become one of the most critical global challenges of the twenty-first century, largely driven by rapid industrialization, population growth, and shifting human lifestyles. Anthropogenic activities—such as industrial production, intensive agriculture, transportation, petroleum exploitation, plastic waste generation, and the widespread use of consumer products—contribute significantly to the continuous release of chemical contaminants into the environment [1–4]. These pollutants adversely affect ecosystems, water quality, soil fertility, and human health, thereby threatening sustainable development. In recent years, particular attention has been directed toward emerging contaminants, which are compounds of anthropogenic origin that are not yet fully regulated but are increasingly detected in environmental matrices. This group includes pharmaceuticals and personal care products (PPCPs), endocrine-disrupting chemicals, alkylphenols, perfluorinated compounds, industrial organic chemicals, and pesticides [5]. Due to their persistence, bioaccumulation potential, and biological activity, these contaminants represent a serious risk to aquatic and terrestrial ecosystems. Pesticides, especially herbicides, are extensively applied worldwide to control weeds and improve agricultural productivity. However, their excessive and uncontrolled use

has led to severe environmental consequences, including soil degradation, loss of biodiversity, and contamination of surface and groundwater resources. Depending on their physicochemical properties, pesticides may undergo biotic and abiotic degradation, adsorb onto soil particles, or leach through the soil profile, ultimately reaching aquatic systems [5,6].Among commonly used herbicides, diuron—a substituted phenylurea compound—stands out due to its high chemical stability, low biodegradability, and strong persistence in the environment. Several monitoring studies have reported the frequent detection of diuron in surface and groundwater. In European rivers, diuron has been detected in nearly 70% of analyzed samples, with concentrations reaching up to 864 ng/L. Regulatory agencies have therefore established strict limits for its presence in drinking water. The European Union sets a maximum allowable concentration of 0.1 µg/L for individual pesticides, while the World Health Organization recommends a guideline value of 4.5 µg/L. Moreover, diuron is classified as a probable human carcinogen by the United States Environmental Protection Agency, raising serious concerns regarding long-term exposure effects on human health [7,8].

To mitigate pesticide contamination, various water treatment and remediation techniques have been developed, including membrane filtration, advanced oxidation processes, ozonation, and biological treatments. Nevertheless, many of these methods are limited by high operational costs, energy consumption, or the generation of hazardous secondary pollutants. In contrast, adsorption is widely recognized as one of the most efficient and economical techniques for water purification due to its operational simplicity, flexibility, and high removal efficiency. A wide range of adsorbent materials has been investigated for diuron removal, including activated carbon, synthetic polymers, and aluminosilicate minerals [9–11]. Among these materials, natural clays have attracted significant interest as low-cost and environmentally friendly adsorbents. Their effectiveness is attributed to their large specific surface area, hydrophilic character, negatively charged surfaces, and cation-exchange capacity. Additionally, clays are abundant, widely available, and require minimal processing, making them suitable for large-scale environmental applications. In this context, Algerian calcic clay represents a promising natural material for pesticide adsorption. While various adsorbents have been extensively studied for pesticide removal, the specific valorization and mechanistic behavior of raw Algerian calcic clay for diuron remediation remain poorly explored in the literature. To bridge this research gap, the present study aims to comprehensively characterize this abundant regional resource and evaluate its efficiency in trapping diuron from aqueous phases. By critically analyzing the effects of key operational parameters alongside rigorous kinetic, isotherm, and thermodynamic modeling, this work provides a thorough understanding of the underlying surface interactions. Ultimately, this comprehensive approach serves to justify the feasibility and economic viability of using this natural local clay for sustainable water treatment applications [1,12–14].

2. Methods

2.1. Materials

The chemicals and reagents used in the present work were of analytical grade and used without further purification. Diuron, sodium hydroxide (NaOH), and hydrochloric acid (HCl) were obtained from Sigma-Aldrich, with NaOH and HCl utilized for adjusting the pH of the aqueous solutions. To determine the specific surface area of the clay, methylene blue dye ($C_{16}H_{18}ClN_3S$) was procured from Sigma-Aldrich. Additionally, barium chloride ($BaCl_2$) and magnesium sulfate (MgSO4) were obtained from the same source and employed specifically for the determination of the clay's Cation Exchange Capacity (CEC). The clay used in our study comes from the Hammam Boughrara deposit. This site is located 25 km northeast of Maghnia and its

current reserves of clay are estimated at 8.2 million tons. The deposit is currently exploited by the national company of non-ferrous mining products and useful substances (ENOF).
Diuron [3-(3,4-dichlorophenyl)-1,1-dimethylurea]; is a phenylated herbicide widely used to control broadleaf weed growth, weeds, mosses and algae. It is generally applied as a pre-emergence and non-selective herbicide in both agricultural and non-agricultural sites. All solutions used in the study were prepared using deionized water [15,16].

2.2.Characterization Methods

The clay material used in this study was previously characterized using several techniques. Fourier-Transform Infrared (FTIR) spectroscopy was performed on a Shimadzu FTIR-8300 spectrophotometer over a frequency range of 400 to 4000 cm^{-1}. X-ray diffraction (XRD) analysis was carried out using a Philips Analytical X'Pert Pro diffractometer operating with copper (λ=1.5418) at a voltage of 45 kV and a current of 40 mA. Morphological observations of the clay surfaces, alongside the qualitative determination of their elemental chemical composition, were conducted via scanning electron microscopy equipped with an energy-dispersive X-ray spectrometer (SEM-EDX) on the powdered sample. Furthermore, the specific surface area was determined using a conductometric method via the Methylene Blue Index [17]. Finally, the Cation Exchange Capacity (CEC), point of zero charge (pHZPC) swelling index, and moisture content of the developed material were systematically determined.

2.3.Adsorption experiments

A stock solution of diuron (31mg/L) was prepared, from which working solutions (2-31 mg/L) were obtained through appropriate dilutions. The influence of various operational parameters on the diuron adsorption efficiency was systematically investigated, including pH (2–12), equilibration time (5–180 min), initial diuron concentration (2-30 mg/L), temperature (293–333 K), and adsorbent mass (0.1–1 g). To evaluate the effect of a single parameter, it was varied while all other variables were kept strictly constant. The residual concentration of diuron in the solution was determined spectrophotometrically at λmax =248nm using a PerkinElmer Lambda 45 UV/Vis spectrophotometer. Finally, the adsorption capacity and removal efficiency of diuron were calculated using Eq. (1) and Eq. (2), respectively.

$$Qads = \frac{C0 - Ceq}{m}.V \quad (1)$$

$$P(\%) = \frac{C0 - Ceq}{C0}.100 \quad (2)$$

With: Qads: Adsorbed quality by gram of the adsorbent in (mg/g) , C_0 : initial concentration in (mg/L), Ceq : concentration at equilibrium in (mg/L), V : Solution volume in (L), m: Adsorbent mass in (g), P(%): Adsorption Percentage.

All adsorption experiments were carried out using the batch equilibration method under carefully controlled conditions to ensure reproducibility and data reliability. The effects of key operational parameters—including pH, contact time, adsorbent dosage, temperature, and initial diuron concentration—were systematically investigated. For each experimental run, a specified

dosage of raw calcium clay was mixed with the diuron solution in Erlenmeyer flasks. The mixtures were continuously agitated using a magnetic stirrer at a constant speed of 700 rpm to maintain a uniform suspension. Following equilibrium, the adsorption data were processed using standard mass balance equations and fitted to various kinetic and isotherm models. The fitting quality of the applied models was evaluated based on their correlation coefficients (R^2). To ensure accuracy, each experiment was performed in triplicate, and the average values were utilized for subsequent data analysis.

3. Results and discussion

3.1.Characterizations

The FTIR spectrum of the pure diuron molecule (Figure1) exhibits two low-intensity absorption bands located at 3280.31 cm^{-1} and 2934.55 cm^{-1}, which are assigned to the stretching vibrations of the N--H bond and the methyl C-H bonds, respectively. In the fingerprint region, several medium-to-strong bands are well-resolved. The prominent band at 1650.37 cm^{-1} is attributed to the C=O stretching vibration [18, 19], while the peaks at 1584.82 cm^{-1} and 1523.57 cm^{-1}correspond to the N-H bending (deformation) and aromatic C=C stretching vibrations, respectively. Furthermore, the bands observed between 1492.51 cm^{-1} and 1358.42cm^{-1} originate from the deformation modes of the methyl C-H bonds. The stretching vibrations of the C-N bonds appear within the 1298.82-1027.40 cm^{-1} range. Finally, the out-of-plane bending vibrations of the aromatic ring C-H bonds are detected between 900.44 cm^{-1} and 813.16 cm^{-1}, whereas the distinct bands in the 755.35-574.56 cm^{-1} region are assigned to the characteristic C-Cl stretching vibrations. Mapping these specific vibrational modes of isolated diuron provides the essential baseline required to track subsequent spectral shifts or intensity changes, which directly elucidate the molecular interactions taking place at the clay-water interface during adsorption.

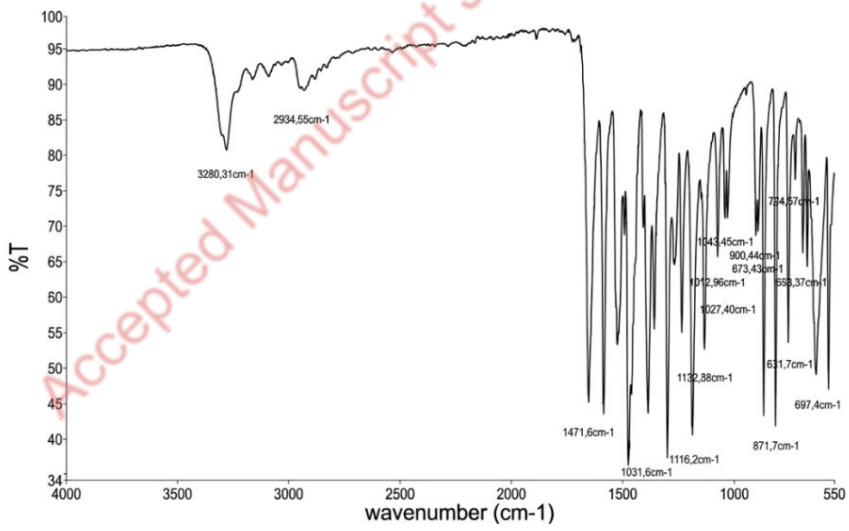

Figure 1. FTIR spectra of Diuron

The FTIR spectra of the raw calcic clay before and after diuron adsorption are illustrated in Figure 2 and Figure 3, respectively. Prior to adsorption, the clay exhibits two low-intensity bands at 3620.90 cm^{-1} and 3382.50 cm^{-1}, which shift slightly to 3620.36 cm^{-1} and 3385.35cm^{-1}

post-adsorption. These signals are assigned to the stretching vibrations of the hydroxyl (-OH) groups from coordinated and physisorbed water molecules. Similarly, the (H-O-H) bending vibration of water molecules shifts from 1631.16 cm^{-1} to 1634.76 cm^{-1} after the process. In the structural framework region, the two intense bands appearing at 983.73 cm^{-1} (983.68 cm^{-1} after adsorption) and 913.76 cm^{-1} (913.19 cm^{-1} after adsorption) are attributed to the stretching modes of the silicate Si-O bonds. The absorption band at 779.17cm^{-1}, which shifts to 792.30 cm^{-1}, characterizes the sharing of -OH groups between octahedral Fe and Al cations. Furthermore, the deformation vibrations of Si-O-Al, Si-O-Mg, and Si-O-Fe linkages are resolved at 693.08 cm^{-1} (693.01cm^{-1}) and 557.43cm^{-1} (575.92cm^{-1}).Comparatively, the overall spectroscopic profile of the calcic clay remains largely unchanged after interaction with the pesticide, preserving its structural integrity. However, the subtle shifts in vibrational frequencies ($\Delta\sigma$), accompanied by minor variations in band intensities, provide clear evidence of weak physical interactions (such as hydrogen bonding and van der Waals forces) between the herbicide and the clay surface. Due to the relatively low maximum adsorption capacity (0.27 mg/g), the characteristic bands of pure diuron such as the N-H stretch around 3200 cm^{-1} and the C=O stretch near 1650 $cm^{-1}$are largely masked by the dominant stretching and bending envelopes of the clay's water molecules, appearing only as subtle, overlapping contributions in the spent adsorbent's spectrum.

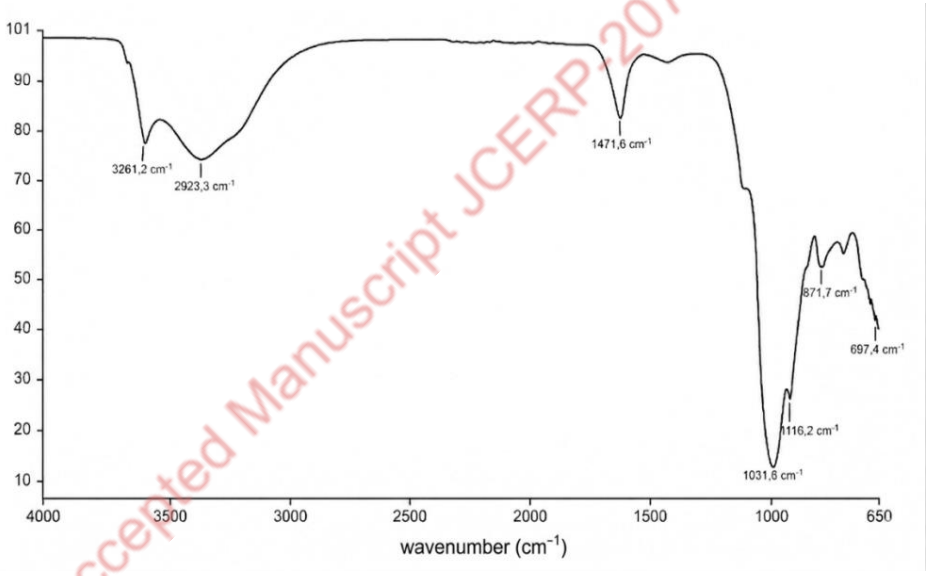

Figure 2. FTIR spectra of Raw Calcium Clay before adsorption

The clay we used in our study is a bentonite rich in montmorillonite, the chemical composition (%by weight) of the calcic clay determined by X-ray fluorescence and quantified in the form of oxides, is represented in Table 1.

Table 1 Chemical composition of the calcic clay

SiO_2	Al_2O_3	Fe_2O_3	CaO	MgO	K_2O	Na_2O

63.44%	12.23%	6.78%	10.3%	1.59%	0.35%	4.18%

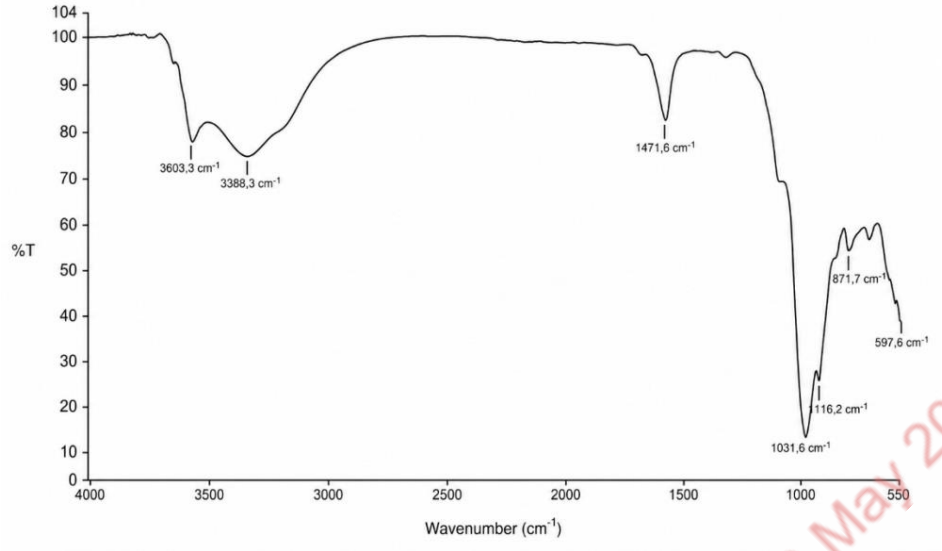

Figure 3. FTIR spectra of Raw Calcium Clay after adsorption

Silica and alumina are the predominant constituent oxides in the studied clay. The SiO_2/Al_2O_3 mass ratio was found to be 4.22, which indicates that the material belongs to the 2:1 bentonite type. This is characteristic of montmorillonite, whose structure consists of an aluminous octahedral sheet sandwiched between two siliceous tetrahedral layers [19, 20]. The cumulative percentage of other minor oxides (Fe_2O_3, MgO, K_2O and Na_2O) reaches 12.88%, confirming the presence of impurities within the clay matrix [21]. Furthermore, the higher content of CaO (10.3%) compared to Na_2O (4.18%) confirms the calcic nature of the bentonite. As detailed in Table 2, the point of zero charge (pHZPC) of the calcic clay is 9.65. Consequently, at pH< pHZPC the clay surface is positively charged, whereas at pH >pHZPC, it becomes negatively charged. The Cation Exchange Capacity (CEC) was determined to be 51.12 meq /100g, which is in good agreement with typical values reported for montmorillonite. Moreover, the swelling index indicates significant interfoliar spacing. The high moisture content highlights the hygroscopic character of the material, confirming its high water adsorption capacity, which is further supported by a large specific surface area (S).The X-ray diffractogram (XRD) of the raw clay is displayed in Figure 4. The measured interplanar distances, d_{hkl}, were assigned to various clay mineral species. Qualitative interpretation of the XRD patterns was carried out by comparing the experimental data with literature standards [4, 22–24]. Quartz was identified as the major crystalline impurity, exhibiting distinct peaks at $2\theta = 20.89°$ and 27°. Conversely, the characteristic reflections observed at $2\theta = 6°$, 19.84°, 29.90° and 36° are attributed to nontronite-15 Å. Finally, sanidine was detected in very low amounts, with weak peaks appearing at 2θ = 23.92°, 26°, 27.89°, and 51° [10, 25].

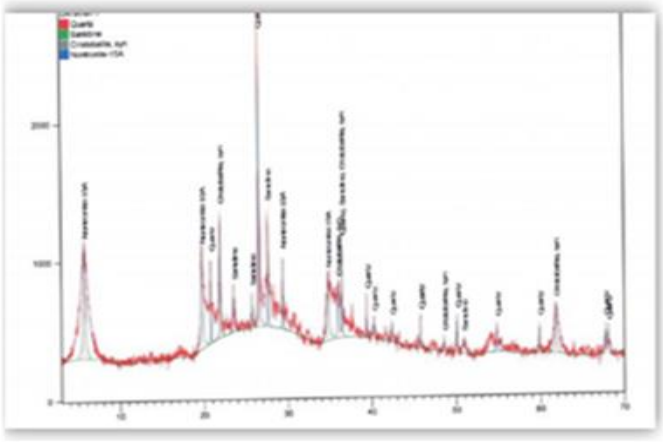

Figure 4. Diffractogram of the raw calcic clay

Table 2 Values of the characteristics of the calcic clay

Characteristics	pHzpc	CEC (meq/100g)	Swelling index	Humidity level	S (m^2/g)
Values	9,65	51,12	2,52	10,46%	640,22

The SEM micrograph of the raw material is displayed in Figure 5. The surface exhibits a highly irregular and porous morphology, indicating that the raw clay possesses an appropriate structure for the effective adsorption of organic pollutants. Furthermore, the elemental composition obtained via EDX analysis is summarized in Table 3. These results are in excellent agreement with those determined by XRF analysis, confirming that the identified elements exist predominantly in their oxide forms. Additionally, the significant proportion of calcium (Ca) further substantiates the calcic nature of the investigated clay [6, 27].

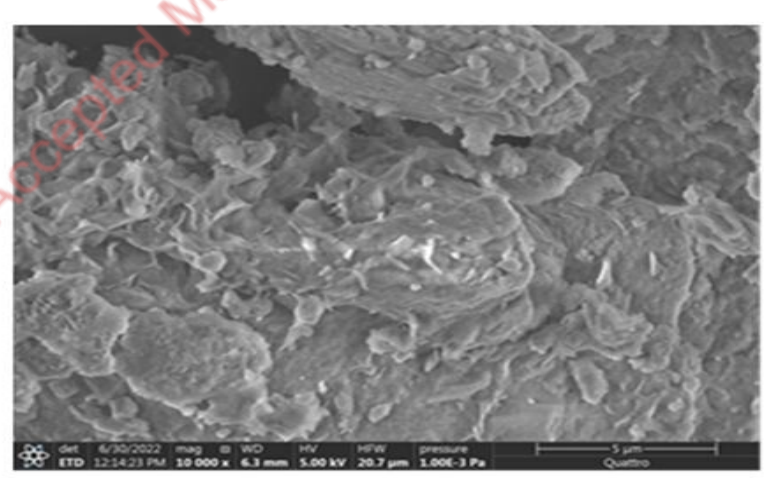

Figure 5. SEM of the raw calcic clay

Table 3 Elemental chemical analysis of raw calcic clay

Element	C	O	Na	Mg	Al	Si	K	Ca	Fe
Weight %	0,00	59.83	1.00	2.50	6.04	17.38	0.45	1.35	3.46

3.2.Optimization of the adsorption parameters of diuron on calcium clay

3.2.1. Effect of contact time

The study of contact time is essential to determine the period required to reach adsorption equilibrium. This experiment was conducted using a series of samples prepared according to the following protocol: 0.5 g of adsorbent was dispersed in 25 mL of a diuron solution 10mg/L) for contact times ranging from 15 to 180 min (Fig. 6). As illustrated in Figure 6, the diuron adsorption percentage on the raw calcic clay increases with longer contact times. The adsorption rate is initially rapid during the early stages of the process, but gradually slows down over time until a plateau is reached. This plateau signifies that adsorption equilibrium has been attained, achieving a maximum removal efficiency of 50% within a contact time of 60 min.

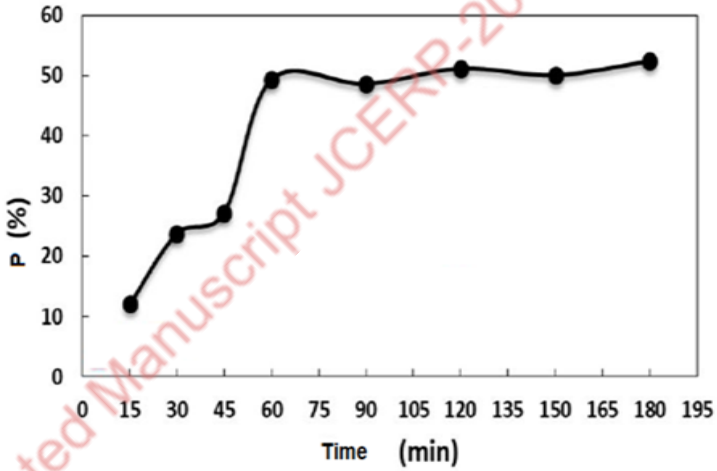

Figure 6. Effect of Time contact on adsorption of Diuron onto calcium clay

3.2.2. Influence of the adsorption mass

To evaluate the influence of adsorbent mass, a series of experiments was conducted by varying the clay dosage. Each mass was placed in contact with 25 mL of a diuron solution (10 mg/L) under constant agitation until equilibrium was reached. The curve illustrating the effect of adsorbent mass is presented in Figure 7. As shown, the removal percentage of diuron by the raw calcium bentonite increases with the increasing mass of the adsorbent. This trend continues until a plateau is reached, achieving a maximum removal efficiency of 39.05%. This stabilization can be attributed to the overlapping or aggregation of adsorption sites at higher clay dosages, which restricts the total available surface area. Consequently, the optimal mass

corresponding to the most effective and efficient removal of diuron was determined to be 0.5 g.

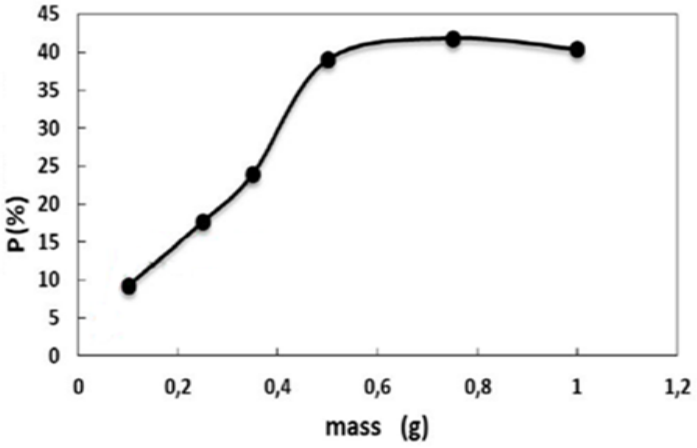

Figure 7. Effect of mass adsorption onto adsorption of diuron onto calcium clay

3.2.3. Influence of the pH

The pH of the solution is a critical parameter in any adsorption study, as it governs both the surface charge of the adsorbent and the ionic structure of the adsorbate. To evaluate the influence of pH on diuron adsorption onto the raw calcic clay, a series of experiments was conducted using a diuron concentration of 10 mg /L across a pH range from 2 to 12. For each test, an adsorbent mass of 0.5 g was introduced into the solution and stirred for 1 h. The initial pH of each solution was precisely adjusted using 0.1M HCl and 0.1 M NaOH solutions. The resulting experimental data are illustrated in Figure 8.

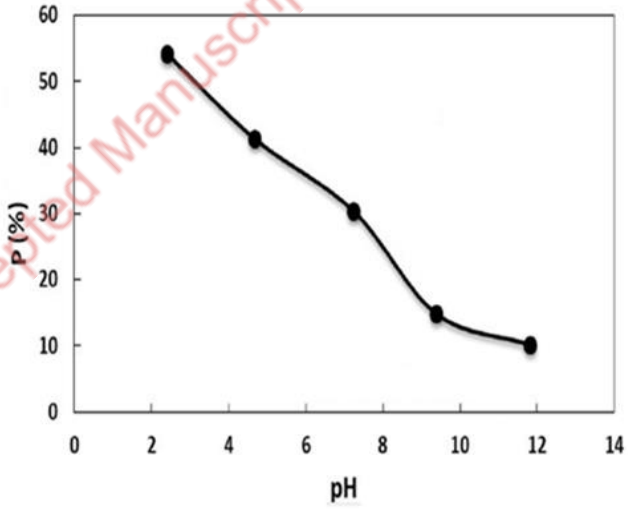

Figure 8. Effect of pH solution on adsorption of Diuron onto calcium clay

The removal percentage of diuron by the raw calcic clay decreases with increasing pH, indicating that the retention process of this herbicide is significantly more favorable in acidic than in alkaline environments. At solution pH values below the pHPZC of the clay, the accumulation of H^+ protons induces a positively charged surface. This surface state promotes

electrostatic attractions with the nucleophilic sites present within the molecular structure of diuron, thereby enhancing adsorption in acidic media. Conversely, at pH values above the pHPZ, the abundance of OH^- anions generates a negatively charged surface environment. This negative charge hinders the approach of diuron molecules due to the scarcity of strong electrophilic sites within the herbicide's structure, ultimately rendering adsorption unfavorable in basic media.

3.2.4. Influence of temperature

The influence of the reaction temperature was investigated by maintaining all previously optimized operational parameters constant for both clay types. Specifically, 25 mL samples of a diuron solution 10 mg/ were introduced into closed flasks containing 0.5 g of clay at an initial pH of 2. Each flask was placed in a temperature-controlled water bath at temperatures ranging from 20 to 60 °C (293–333 K) under constant agitation for 1 h. The graphical plot of the removal percentage as a function of temperature is presented in Figure 9. The experimental profile clearly demonstrates that temperature variations have a negligible effect on the diuron adsorption process onto the raw calcic clay.

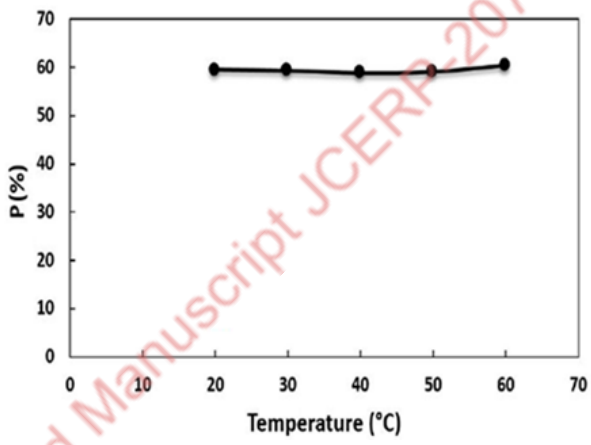

Figure 9.Effect of temperature on adsorption of diuron

The calculation of the differential adsorption heats of diuron on clay for various degrees of surface coverage is intended to determine the isosteric heat of adsorption. This thermodynamic quantity is a parameter that determines whether adsorption is physical or chemical. Thermodynamic parameters such as the free enthalpy ΔG, the enthalpy ΔH, and the entropy ΔS were determined using the following equations

$$Kd = \frac{Qe}{Ce} \qquad (3)$$

$$\Delta G = -RT \ln Kd \qquad (4)$$

$$LnKd = \left(\frac{\Delta S}{R}\right) - \left(\frac{\Delta H}{R}\right)\frac{1}{T} \qquad (5)$$

where: kd: Distribution coefficient for adsorption. kd = Qe/Ce, ΔS and ΔH: Changes in entropy and enthalpy of adsorption, ΔG: Free enthalpy or Gibbs energy of adsorption, R: Ideal gas

constant, T: Absolute temperature of the isotherm (in K), Qe: Equilibrium adsorption capacity ($mg \cdot g^{-1}$), Ce: Equilibrium concentration of the solute in solution (mg/L).

The variation of ln kd as a function of 1/T allowed us to deduce the thermodynamic parameters for the adsorbent/adsorbate systems under study. And the results are summarized in the table

Table 4 Thermodynamic parameters of diuron adsorption on activated calcium clay.

ΔH (kJ/mol)	ΔS (kJ/mol.K)	T (K)	ΔG (Kj/mol)
-6,824	0,05006	303	8,345695
		313	8,846345
		324	9,397061

The negative values of ΔH ° confirm the exothermic nature of the adsorption process, while its low magnitude (<40 kJ/mol) clearly indicates a physisorption mechanism governed by weak physical interactions [33]. Regarding the entropy change ΔS, the low positive value observed for the activated calcium clay reflects an increase in randomness at the solid-solution interface, typically caused by the displacement and release of water molecules from the clay surface; conversely, the negative ΔS value for the raw calcium clay demonstrates a decrease in randomness, indicating that the adsorption occurs with an increase in structural order as diuron molecules become immobilized on the surface [34]. Furthermore, for both clays, the Gibbs free energy ΔG increases with rising temperature, proving that the process becomes thermodynamically less favorable and non-spontaneous at higher temperatures; this endothermic evolution ΔG is consistent with the exothermic nature of the system $\Delta G = \Delta H - T\Delta S$, where thermal agitation disrupts the weak physisorption bonds and triggers a redistribution of energy between the adsorbent and the adsorbate [35].

3.2.5. Adsorption isotherm

Adsorption isotherms are essential tools for elucidating adsorption mechanisms and evaluating the suitability of an adsorbent for large-scale applications. In this study, adsorption isotherm experiments were conducted by varying the initial diuron concentration from 5 to 31 mg/L1. As illustrated in the graphical plot of qe versus Ce (Figure 10), the equilibrium adsorption capacity (qe) increases progressively with the increase in equilibrium diuron concentration (Ce). The maximum adsorption capacity was determined to be 0.27mg/g. This continuous increase in the adsorption capacity without reaching a strict horizontal plateau suggests the formation of multilayer coverage, thereby confirming that physisorption is the dominant mechanism governing the diuron removal process onto the raw calcic clay.

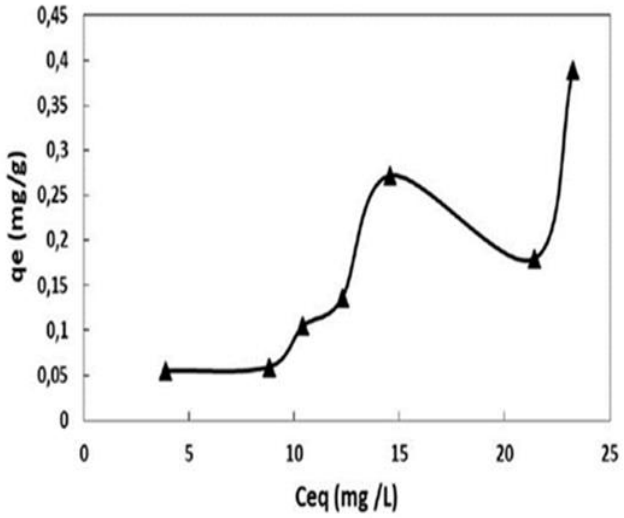

Figure 10. Adsorption isotherm of diuron

3.2.6. Comparison with Other Adsorbents

To evaluate the performance of the raw calcic clay, its maximum diuron adsorption capacity was compared with various adsorbents reported in the literature (Table 5). The determined adsorption capacity (0.27 mg/g) is relatively lower than those of activated carbons or chemically modified/synthesized materials. This limitation is primarily attributed to the raw and unmodified nature of the natural bentonite, which lacks highly developed synthetic porosities or specific functional anchors that artificial materials possess.However, from an industrial and environmental standpoint, the use of this raw clay offers significant competitive advantages. Unlike commercial activated carbons or chemically functionalized clays, this material requires no expensive, time-consuming, or energy-intensive thermal/chemical pre-treatments. It is locally abundant, completely non-toxic, and boasts a near-zero preparation cost. Therefore, while its absolute adsorption capacity is modest, its exceptional cost-effectiveness and ecological sustainability render it a highly viable and attractive "green" alternative for the decentralized treatment of pesticide-contaminated water.

Table 5: Comparison of maximum diuron adsorption capacities of various adsorbents.

dsorbent	**qmax (mg/g)**	**Chemical Modification**	**Reference**
Commercial Activated Carbon	50.0 – 150.0	High thermal/chemical activation	[6]
Acid-activated Bentonite	4.5 – 12.0	Concentrated H_2SO_4 / Or HCl treatment	[7]

dsorbent	qmax (mg/g)	Chemical Modification	Reference
Organo-modified Montmorillonite	8.0 – 25.0	Surfactant intercalation (CTAB, etc.)	[5]
Raw Calcic Clay (Algeria)	**0.27**	**None (Raw natural state)**	**This work**

3.2.7. Modeling of isotherms

Several two-parameter mathematical models have been tested to model the adsorption isotherms of diuron on clay, we can mention the models of Freundlich (6), Langmuir (7), Temkin (8) and Elovich (9).

$$\text{Ln } q_e = \ln K_F + \frac{1}{n} \ln C_e \quad (6)$$

$$\frac{1}{q_e} = \frac{1}{C_e} \frac{1}{q_m K_L} + \frac{1}{q_m} \quad (7)$$

$$q_e = B_1 \ln K_t + B_1 \ln C_e \quad (8)$$

$$q_t = \frac{1}{\beta} \ln(\alpha\beta) + \frac{1}{\beta} \ln t \quad (9)$$

With : qe : quantity of solute adsorbed per unit mass of the adsorbent at equilibrium (mg/g), qt : quantity of solute adsorbed per unit mass of the adsorbent at equilibrium (mg/g), K_F : Freundlich constant associated with the adsorption capacity, qm : represents the maximum adsorption capacity (mg/g), K_L : equilibrium constant, equal to the ratio of adsorption and desorption rates (L/mg), t : the time (min), K_E : the equilibrium constant of Elovich (L/mg), B_1=RT/b_t (J/mol), the Temkin constant for the heat of sorption and Kt (L /g)), the equilibrium constant of adsorption corresponding to the maximum binding energy.

Table 6 Adsorption parameters of the diuron onto calcic clay

Models	Constantes	Valeurs
Freundlich	R^2	0,9847
	n	1,41
	K_F(mg/g) $(L/mg)^{1/n}$	0,0212

Langmuir	R^2 Q_m (mg/g) K_L (L/mg) R_L	0,9892 0,33 0,051 0,495
Temkin	R^2 B_t (kJ/mol) K_T (L/mol)	0,9585 0,0723 0,51
Elovich	R^2 Q_m (mg/g) K_E (L/mg)	0,8254 0,265 0,0633

To evaluate the equilibrium relationship and understand the surface properties of the adsorbent, the experimental data were fitted using linear regression analysis across four established isotherm models: Langmuir, Freundlich, Temkin, and Elovich. The applicability of each model was rigorously evaluated based on the determination coefficient (R^2) as the primary metric to demonstrate fitting rationality. As summarized in Table 6, both the Langmuir (R^2 = 0.9892$) and Freundlich ($R^2$ = 0.9847) models yielded exceptionally high and remarkably close correlation coefficients.Rather than an inconsistency, this dual mathematical validity reflects a complex, two-step cooperative adsorption mechanism occurring on the heterogeneous surface of the raw Algerian clay. At lower equilibrium concentrations, diuron molecules are preferentially accommodated onto the highly energetic and accessible structural active sites of the calcic bentonite. This initial phase leads to the formation of a localized monolayer (monocouche), perfectly satisfying the Langmuir criteria: adsorption onto a finite number of homogeneous sites without lateral interactions. The physical significance of this first stage is quantified by a maximum monolayer adsorption capacity (Qm) of 0.33 mg/g and a Langmuir affinity constant (K_L) of 0.051 L/mg. Furthermore, the rationality of this model is validated by the dimensionless separation factor (R_L = 0.495), which confirms a highly favorable process (0 < R_L < 1).As the initial active sites approach saturation at higher equilibrium concentrations, the adsorption profile transitions into a second phase characterized by a multilayer formation (multicouche). Once the first layer is complete, the already adsorbed diuron molecules act as secondary templates, attracting further solute molecules via weaker solute–solute physical interactions, such as hydrogen bonding and van der Waals forces. This second stage is accurately captured by the Freundlich model. The derived physical intensity parameter (n = 1.41) lies well within the favorable range (1 < n < 10), mutually supporting the physisorption nature of this multilayer accumulation. Conversely, the lower correlation coefficients of the Temkin (R^2 = 0.9585) and Elovich (R^2 = 0.8254) models indicate their limited overall applicability to this system. Specifically, the Temkin heat of adsorption parameter (Bt = 0.0723Kj/mol) yields a very low value, which physically substantiates that the entire system is

governed by weak physical forces rather than chemical bonding. Consequently, the simultaneous statistical validity of the Langmuir and Freundlich models conclusively demonstrates that diuron retention onto this raw natural clay is a sequential process, evolving from an initial energetic monolayer anchoring to a subsequent physisorbed multilayer stacking [28].

3.2.8. Adsorption kinetics

Several kinetic models were used to interpret the experimental data, providing essential information for the application of these two types of clay in the field of adsorption. We employed five kinetic models: These models are: pseudo-first-order (10), pseudo-second-order (11), intraparticle diffusion (12), external diffusion (13), and Elovich models (14).

$$\ln(q_e - q_t) = \ln q_e - k_1 t \quad (10)$$

$$\frac{1}{q_t} = \frac{1}{K_2 q_e^{\,2}} + \frac{1}{q_e} t \quad (11)$$

$$q_t = K_p . t^{1/2} \quad (12)$$

$$Ln\left[\left(\frac{C0 - Ce}{Ct - Ce}\right)\right] = K' t \quad (13)$$

$$qt = \frac{1}{\beta} \ln(\alpha\beta) + \frac{1}{\beta} \ln t \quad (14)$$

The kinetic data for diuron adsorption onto calcium clay were evaluated using several models to elucidate the rate-controlling steps. The experimental equilibrium adsorption capacity (qe=0.41mg/g) aligned remarkably well with the calculated capacity qe cal derived from the pseudo-first-order model, which also yielded a coefficient of determination (R2) close to unity (Table 7). This excellent agreement confirms that the adsorption kinetics of diuron are governed by the Lagergren pseudo-first-order model, ruling out the pseudo-second-order mechanism due to the significant discrepancy between its calculated and experimental qe values. Furthermore, the low R2 value obtained from the Elovich kinetic model reinforces the non-chemical nature of the process, confirming that diuron uptake does not involve chemisorption. Regarding mass transfer resistance, the intraparticle diffusion step was found not to be the sole rate-limiting stage but rather coupled with external film diffusion. This prominent role of external mass transfer was confirmed by the high regression coefficient (R2 = 0.95) obtained from the linearization of ln[(C0 - Ce)/(Ct - Ce)] versus contact time, definitively establishing that boundary layer (external) diffusion represents a major rate-determining step in the overall adsorption process. The experimental results exhibited good consistency and reproducibility throughout the adsorption study. The relatively high correlation coefficient values obtained for the applied adsorption models indicated a satisfactory agreement between the experimental and theoretical data. This confirms the reliability of the experimental methodology and supports the suitability of the selected models for describing the adsorption behavior of diuron onto raw Algerian calcic clay.

Table 7 constant values of the kinetic models studied

kinetic model	Constants	Calcic clay
External distribution	R^2	0.9491
	K' (cm^3 /L)	0.0308
Intraparticle diffusion	R^2	0.9718
	K_w (min^{-1})	0.04
Pseudo-first order	R^2	0.9526
	q_e (mg/g)	0.4457
	K_1 (min^{-1})	0.0322
Pseudo-second order	R^2	0.8916
	K_2 (min^{-1})	0.056
	q_e (mg/g)	0.511
Elovich	R^2	0.8926
	α_E (mg/g.min)	0.038
	β_E (g/mg)	10.03

4. Conclusion

This study demonstrates the strong potential of an abundant natural clay from Algeria for the efficient removal of diuron from groundwater and surface water. The experimental results highlight the critical role of the adsorbent's characteristics—particularly those of calcium montmorillonite—in governing the overall adsorption process. The influences of exchangeable cations and solution pH were found to be highly significant, emphasizing the importance of physicochemical interactions between diuron molecules and the clay surface. A detailed investigation of the underlying mechanisms revealed that diuron retention on montmorillonite is controlled by a synergetic combination of processes, including cation exchange, electrostatic interactions, and surface affinity. The determined adsorption capacities confirm that diuron can be effectively removed using raw natural clay without the need for chemical modification, representing a major advantage in terms of cost-effectiveness and environmental sustainability. Overall, calcium bentonite emerges as an efficient, low-cost, and eco-friendly adsorbent for the treatment of pesticide-contaminated water. This work provides valuable insights into the development of sustainable water treatment strategies utilizing locally available resources and contributes to the advancement of green solutions for water pollution control.

Acknowledgement

We would like to express our sincere gratitude to the Directorate General for Scientific Research and Technological Development (DGRSDT) and the Algerian Ministry of Higher Education and Scientific Research (MESRS), as well as the Materials and Catalysis Laboratory, Faculty of Exact Sciences, Djilali Liabes University, Sidi Bel Abbes, Algeria.

REFERENCES

[1] Deng, Jing., Shao, YiSheng., Gao, NaiYun., Deng, Yang.,Tan, ChaoQun., Zhou, ShiQing., Hu, XuHao. (2013). Multiwalled carbon nanotubes as adsorbents for removal of herbicide diuron from aqueous solution. Chem. Eng. J, 193, 339-347. DOI.org/10.1016/j.cej.2012.04.051

[2] Yankui, T., Xiaoyu, P., Weiwei, Y., Yue, Z., Maozhong, Y., Yan, L., Zhanfeng, D. (2017). Emerging Pollutants – Part I: Occurrence. Fate and Transport. Water Environ Res, 89 (10), 1810-1828. DOI.org.10.2175/106143017X15023776270665

[3] Dedi, T., Sri, R. W., Nita, P. S., Vida, E., Livia, R. A., Adityas, A. R. (2025). Cellulose Xanthate–alginate Beads from Empty Palm Fruit Bunches: Synthesis, Characterization, and Application in Remazol Red Dye Degradation, Perio. Poly.Chem. Engi, 69 (4), 510-524. DOI.org/10.3311/PPch.42243.

[4] Nayoon, C., Yeongkyun, S., Tae-Hyun, K., Yuri, P., Yuhoon, H. (2023). Adsorption behaviors of modified clays prepared with structurally different surfactants for anionic dyes removal. Environ. Eng. Res. 2023; 28(2): 220076. DOI.org/10.4491/eer.2022.076

[5] Stefano, S., Jelena, J., Borivoj, A. (2016). Comparison of adsorbent materials for herbicide Diuron removal from water. *Desalin and Water Treat,* 57, 1876-1888. DOI.org/10.1080/19443994.2016.1180484

[6] Roberto, D., Rachel, C., Gerardo, G., Chiara, F. (2015). Diuron in water: Functional toxicity and intracellular detoxification patterns of active concentrations assayed in tandem by a yeast-based probe. Int. J. Environ. Res. Public Health, 12 (4), 3731-3740. DOI.org.10.3390/ijerph120403731.

[7]Stefano, S. (2013). Diuron herbicide degradation catalyzed by low molecular weight humic acid-like compounds. Environ. Chem. Lett, 11, 359–363. DOI.org/10.1007/s10311-013-0415-5

[8] Nomcebo, H., Mthombeni, S. M., Maurice, S. O. (2010). . Magnetic zeolite-polymer composite as an adsorbent for the remediation of waste- waters containing vanadium. Int. J. Environ. Sci. Dev, 6(8), 657-666. DOI.org10.7763/IJESD.2015.V6.665

[9] Olugbenga, S. B., Isah, A. B., Kayode, A. A., (2013). Adsorption of dyes using different types of sand. review, S. Afr. J. Chem,66, 117-129. DOI.journals.sabinet.co.za/sajchem

[10] Maqueda, C., dos Santos, A., Morillo, E., Torres, S., P, S., Undabeytia, T. (2013). Adsorption of diuron on mechanically and thermally reated montmorillonite and sepiolite. Appl. Clay Sci, 72, 75-183. DOI.org/10.1016/j.clay.2012.10.017.

[11] Ruta, O., Andrejs, K., Juris, B., Maris, K., Zane, V.G. (2024). Surfactant-Modified Clay Sorbents for the Removal of p-nitrophenol, Clays. And. Mine. Clay, 67,132-142. DOI.org/10.1007/s42860-019-00015-2

[12] Laurance, E., Haither Hellar, K., Quintino, A.M., Esther, H.J. (2023). Comparative analysis of cationic dye adsorption efficiency of thermally and chemically treated. Tanzanian kaolin, 82,101. DOI.org/10.1007/s12665-023-10782-w.

[13] Chargui, H., Hajjaji, W., Johan, Y. (2018). Direct Orange 34 dye fixation by modified kaolin. Clay Minerals, 53, 271-287. DOI.org/10.1180/clm.2018.18

[14] Nóra, H., Richárd, T., Béla, P. (2017). Determination of the specific surface area of layered silicates by methylene blue adsorption: The role of structure, pH and layer charge. Applied Clay Science, 149, 50-55. DOI.org/10.1016/j.clay.2017.05.007

[15] Alfian, P., Rizal, S., Teuku, R., Nurhanifa, A. (2021). Removal of hg(ii) metal ions using kaolin adsorbents modified with anionic surfactant and efficient ultrasonic assisted. Inter.Jou. of Resea .Grath, 9 (11). DOI.org/10.29121/granthaalayah.v9.i11.2021.4379

[16] Leonid, P., Maria, G., Maria, B., Hemalatha, S., Irina, P., Yury, H. (2024). Organoclays Based on Bentonite and Various Types of Surfactants as Heavy Metal Remediants. Sust.,(11), 4804. DOI.org/10.3390/su16114804

[17] Pentrák, M., Czímerová, A., Madejová, J., Komadel; P. (2012). Changes in layer charge of clay minerals upon acid treatment as obtained from their interactions with methylene blue. J. Applie. Clay. Scien. 55, 100-127. https://doi.org/10.1016/j.clay.2011.10.012.

[18] Muthanna, J.A., Samar, K. D. (2012). Equilibrium isotherms and kinetic modeling of methylene blue adsorption on agricultural wastes-based activated carbons. J.Fluid Phase Equilibria 317, 9-14. DOI.org/10.1016/j.fluid.2011.12.026

[19] Maria, G., Leonid, P., Anna, K., Marina, B., Yury, H. (2024). Removal of Lead Cations by Novel Organoclays Derived from Bentonite and Amphoteric and Nonionic Surfactants. Toxics, 12,713.DOI.org/10.3390/toxics12100713

[20] Perera, M.D.R., Amarasena, R.A., Bandara, A.T., Weerasooriya, R., Jayarathna, L. (2023). Surfactant-Modified Clay Composites : Water Treatment Applications. Clay Comp,233-252. DOI.org/10.1007/978-981-99-2544-5_11

[21] Qlihaa, A., Dhimni, S., Melrhaka, F., Hajjaji, N, Srhiri, A. (2016). Caractérisation physico-chimique d'une argile Marocaine. J. Mater. Environ. Sci, 7(5) , 1741-1750. DOI. www.jmaterenvironsci.com

[22] Guang-Cai, C., Xiao-Quan, Shan., Zhi-Guo, Pei., Huanhua, Wang., Li-Rong, Zheng., Jing, Zhang., Ya-Ning, Xie. (2011). Adsorption of diuron and dichlobenil on multiwalled carbon nanotubes as affected by lead. J. Hazard. Mater, 188, 156-163. DOI.org/10.1016/j.jhazmat.2011.01.095

[23] Sunil, K., Deokar, S., A. Mandavgane , A. (2015). Rice husk ash for fast removal of 2,4-Dichlorophenoxyacetic acid from aqueous solution. Adsorp. Sci. Technol, 429-440. DOI.org/10.1260/0263-6174.33.5.429

[24] Sunil, D., Ganesh, B.G.B., Payal, B., Sachin, A.M. (2017). Adsorptive Removal of Diuron Herbicide on Carbon Nanotubes Synthesized from Plastic Waste. Journal of Environmental Polymer Degradation, 25, 165-175. DOI.org.10.1007/s10924-016-0794-3

[25] Chandra, M., Priyanka. K., Rajender, S. V., Neeraj, K. (2026). Clay surface modification with cationic surfactant and their thermal, morphological and crystal structure analysis. Resu.in Chem, 24, 103183. DOI.org/10.1016/j.rechem.2026.103183.

[26] Mohamed, Z., Kaisu, A., Zouhair, E., Satu, O., Nadia, E., R, L. K., Mohammed, B., Rachid, Brahmi. (2018). Steam activation of waste biomass: highly microporous carbon, optimization of bisphenol A, and diuron adsorption by response surface methodology. Environ. Sci. Pollut. Res. 25, 35657-35671. DOI.org/10.1007/s11356-018-3455-3

[27] Selvakumar, P., Saravanan, R., Vivek, K. C., Jagadeeswari, R.,Karthikeyan, R. (2025). Application of Response Surface Methodology for the Adsorptive Removal of Chromium Using Modified Cellulose. Perio. Poly. Chem. Engi. 69(4), 545-558. DOI.org/10.3311/PPch.41153

[28] Rita, M., Éva, F., Lajos, S., István, K., Mónika, M. (2025). Impact of Randomly Methylated Cyclodextrins on Candida albicans: Biofilm Formation, Morphogenesis and Oxidative Stress. Perio. Poly.Chem. Engi,69 (4), 501-509. DOI.org/10.3311/PPch.41530